atmosphere

MDPI

Article

Inverse Relations of $PM_{2.5}$ and O_3 in Air Compound Pollution between Cold and Hot Seasons over an Urban Area of East China

Mengwei Jia [1], Tianliang Zhao [1,*], Xinghong Cheng [2,*], Sunling Gong [2], Xiangzhi Zhang [3], Lili Tang [3], Duanyang Liu [4], Xianghua Wu [5], Liming Wang [5] and Yusheng Chen [1]

1 Collaborative Innovation Center on Forecast and Evaluation of Meteorological Disasters, Key Laboratory for Aerosol-Cloud-Precipitation of China Meteorological Administration, Nanjing University of Information Science and Technology, Nanjing 210044, China; jiamengwei8822@163.com (M.J.); cyseverglow@163.com (Y.C.)
2 State Key Laboratory of Severe Weather, Institute of Atmospheric Composition, Chinese Academy of Meteorological Sciences, Beijing 100081, China; sunling@camscma.cn
3 Jiangsu Provincial Environmental Monitoring Center, Nanjing 210029, China; zhangxzhzz@126.com (X.Z.); lily3258@163.com (L.T.)
4 Jiangsu Provincial Meteorological Observatory, Nanjing 210008, China; Liuduanyang2001@126.com
5 School of Mathematics and Statistics, Nanjing University of Information Science and Technology, Nanjing 210044, China; wuxianghua@nuist.edu.cn (X.W.); wanglimingnuist@163.com (L.W.)
* Correspondence: tlzhao@nuist.edu.cn (T.Z.); cxingh@cma.gov.cn (X.C.)

Academic Editor: Yuxuan Wang
Received: 14 February 2017; Accepted: 16 March 2017; Published: 20 March 2017

Abstract: By analyzing the data of urban air pollutant measurements from 2013 to 2015 in Nanjing, East China, we found that the correlation coefficients between major atmospheric compound pollutants $PM_{2.5}$ and O_3 were respectively 0.40 in hot season (June, July and August) and −0.16 in cold season (December, January and February) with both passing the confidence level of 99%. This provides evidence for the inverse relations of ambient $PM_{2.5}$ and O_3 between cold and hot seasons in an urban area of East China. To understand the interaction of $PM_{2.5}$ and O_3 in air compound pollution, the underlying mechanisms on the inversion relations between cold and hot seasons were investigated from the seasonal variations in atmospheric oxidation and radiative forcing of $PM_{2.5}$ based on three-year environmental and meteorological data. The analyses showed that the augmentation of atmospheric oxidation could strengthen the production of secondary particles with the contribution up to 26.76% to ambient $PM_{2.5}$ levels. High O_3 concentrations in a strong oxidative air condition during hot season promoted the formation of secondary particles, which could result in a positive correlation between $PM_{2.5}$ and O_3 in hot season. In cold season with weak atmospheric oxidation, the enhanced $PM_{2.5}$ levels suppressed surface solar radiation, which could weaken O_3 production for decreasing ambient O_3 level with the low diurnal peaks. Under the high $PM_{2.5}$ level exceeding 115 $\mu g \cdot m^{-3}$, the surface O_3 concentration dropped to 12.7 $\mu g \cdot m^{-3}$ at noon with a significant inhibitory effect, leading to a negative correlation between $PM_{2.5}$ and O_3 in cold season. This observational study revealed the interaction of $PM_{2.5}$ and O_3 in air compound pollution for understanding the seasonal change of atmospheric environment.

Keywords: $PM_{2.5}$; O_3; air compound pollution; urban area

1. Introduction

With the rapid economic development and accelerating urbanization process, a lot of energy is consumed, increasingly releasing pollutant emissions into ambient air in urban regions of

China, where air pollution has been changing from coal-smoke to compound-polluted type. Air compound pollution brings serious environment and health problems in urban areas of China [1,2]. As representative pollutants of air compound pollution, ozone (O_3) and fine particles ($PM_{2.5}$) in ambient atmosphere, are becoming a pervasive air quality problem facing China. The urban regions in the Yangtze River Delta of East China, Beijing-Tianjin-Hebei region of the North China Plain, the Pearl River Delta of South China and the Sichuan Basin of Southwest China are particularly acute [3–7]. With a high density of population, the prosperity of industrial activity and transportation, Nanjing, a major urban area in Yangtze River Delta region, has also been experiencing air compound pollution in recent years [8–10].

Ambient O_3 pollution, known as photochemical smog, is generated through a series of complex photochemical reactions related to oxides of nitrogen (NO_x) and volatile organic compounds (VOC) under strong solar radiation. Photochemical smog and haze pollution generally take place simultaneously with the interaction between O_3 and $PM_{2.5}$ for air compound pollution [11]. The interaction between O_3 and $PM_{2.5}$ is mainly affected by the photochemical reaction [12]. In ambient atmosphere, O_3 photolysis generates OH, and then OH oxidizes VOCs to promote NO conversion to break the steady-state relationship. Photochemical reactions are an important source of tropospheric O_3. In addition to photochemical reactions, the heterogeneous reactions occurring on the surface of soluble particulate matter and black carbon are also an important way for the interaction between O_3 and atmospheric particles [13–16]. Li et al., analyzed the data collected from Diffuse Reflectance Infrared Fourier Transform Spectroscopy (DRIFTS) and reported that in the presence of O_3, SO_2 could be oxidized to sulfate on the surface of $CaCO_3$ particles [17]. Ge et al., found that high concentrations of NO_x can largely enhance the formation of nitrate in fine particles under high O_3 and the favorable meteorological conditions [18]. Secondary organic and inorganic aerosols generated from oxidation reactions comprise a significant fraction of particulate matters with high implications for air pollution in China [19].

Generally, aerosols or atmospheric particles alter the earth's radiation budget through aerosol direct and indirect radiative forcing [20]. Zhu et al., and Xu et al., used a box model and a three-dimensional regional chemical transport model to evaluate the impact of dust particles on tropospheric photochemistry over Beijing megacity with high dust concentrations leveling down the ambient O_3 [21,22]. Feng et al., (2015) analyzed the summertime O_3 formation in a megacity in Northwest China and concluded that high concentrations of particulate matters can decrease the photolysis frequencies significantly with reduced O_3 by more than 50 $\mu g \cdot m^{-3}$ (around 25 ppb) [23]. However, a positive correlation between $PM_{2.5}$ and O_3 with a coefficient $R = 0.24$ is found in summer over Hangzhou, a coastal city in East China [8]. Obviously, air pollution could be more complicated with the interaction between $PM_{2.5}$ and O_3, which needs to be further investigated.

Previous studies on interaction between $PM_{2.5}$ and O_3 mostly focused on individual seasons and air pollution episodes, and the comprehensive mechanism between $PM_{2.5}$ and O_3 in air compound pollution has been poorly understood. Based on three-year (2013–2015) environmental and meteorological monitoring data in Nanjing, a major urban area in East China, this study attempted to comprehensively explore the relation of $PM_{2.5}$ and O_3 and its seasonal change to deepen the understanding of air compound pollution in China with the implications on atmospheric environment changes.

2. Environmental and Meteorological Data

Nanjing—the capital city of Jiangsu Province in East China (left panel of Figure 1) with a population of 8.18 million—is the urban area for our study. In this study, we analyzed the hourly environmental monitoring data from 1 January 2013 to 31 December 2015 at nine state sites covering the urban area of Nanjing. The Environmental monitoring data included the hourly surface particle mass concentrations of $PM_{2.5}$ and PM_{10} as well as Ozone (O_3), carbon monoxide (CO), sulfur dioxide (SO_2) and nitrogen dioxide (NO_2). To analyze the interaction between $PM_{2.5}$ and O_3 in this study,

the hot and cold seasons were climatologically defined from June to August and from December to the following February respectively for the East Asian summer and winter monsoon seasons in this urban area over East China [24].

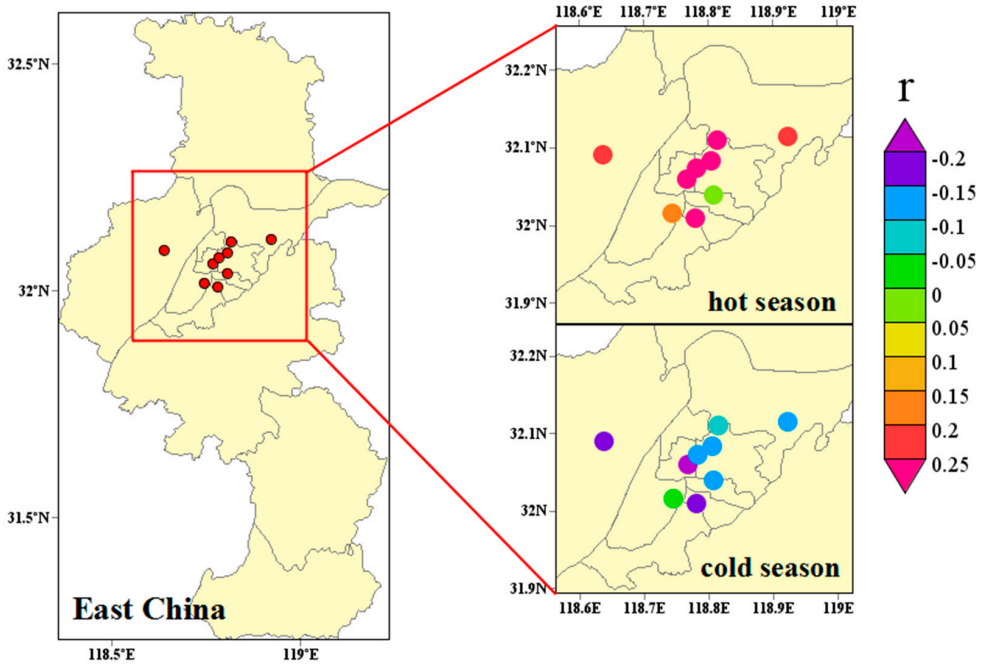

Figure 1. The geographic locations of 9 state controlling air sampling sites in the urban area of Nanjing in East China (**left panel**) with the correlation coefficients between ambient fine particles ($PM_{2.5}$) and ozone (O_3) in hot and cold seasons in the urban area of Nanjing over 2013–2015 (**right panel**).

The correlation coefficients between $PM_{2.5}$ and O_3 at the urban sites in hot and cold seasons were presented in the right panels of Figure 1. Interestingly, the positive and negative correlations were observed respectively in hot and cold seasons over three years of 2013–2015 (right panel of Figure 1). Averaged over nine air sampling sites in the urban area, the correlation coefficients between $PM_{2.5}$ and O_3 in hot and cold seasons were respectively reaching to 0.40 and −0.16 with both passing the confidence level of 99%, revealing the inverse relations of ambient $PM_{2.5}$ and O_3 between cold and hot seasons in an urban area of East China.

The meteorological data of surface air temperature and total radiation observed at Nanjing observatory over 2013–2015 were also used to analyze the seasonal variation of meteorological condition in this study. Based on the environmental and meteorological data, the underlying mechanisms of inversion relations between ambient $PM_{2.5}$ and O_3 in cold and hot seasons were explored to understand the seasonal variations in air compound pollution in the following sections.

3. Analysis and Discussion

Air quality change could be complex, resulting from the interaction between $PM_{2.5}$ and O_3 in air compound pollution [25]. In this section, we examined the seasonal changes of atmospheric environment and meteorological condition to interpret the underlying mechanisms of inversion relations of $PM_{2.5}$ and O_3 between cold and hot seasons for understanding on the interaction of $PM_{2.5}$ and O_3 in atmospheric environment change.

3.1. Seasonal Variations of Atmospheric Environment and Meteorological Conditions

Ambient $PM_{2.5}$ and O_3 levels are dominant in haze and photochemical air pollution for air quality change over China [11]. In this study, the light, moderate and heavy levels of haze pollution were

ranked with daily $PM_{2.5}$ concentrations from 35 to 75 $\mu g \cdot m^{-3}$, from 75 to 115 $\mu g \cdot m^{-3}$, and exceeding 115 $\mu g \cdot m^{-3}$, and the light, moderate and heavy levels of photochemical air pollution were ranged with the daily maximum O_3 concentrations varying between 100 and 160 $\mu g \cdot m^{-3}$, between 160 and 200 $\mu g \cdot m^{-3}$ and higher than 200 $\mu g \cdot m^{-3}$. Based on the $PM_{2.5}$ and O_3 measurements from 2013 to 2015 over the urban area of Nanjing, we could calculate the proportions of the light, moderate and heavy levels of haze and photochemical air pollution in cold and hot seasons during three years with the following formula:

$$\text{Proportion} = N/TD \times 100\% \quad (1)$$

with N representing the number of polluted days in each air pollution level in cold or hot seasons, and TD standing for the total days of same air pollution level during cold and hot seasons over 2013–2015. The proportions calculated with Equation (1) could reflect the seasonal variations in atmospheric environment connecting with $PM_{2.5}$ and O_3 pollution over the urban area in cold and hot seasons (Tables 1 and 2).

Table 1. The proportions of three $PM_{2.5}$ levels ($\mu g \cdot m^{-3}$) in cold and hot seasons in the urban area of Nanjing over 2013–2015.

Seasons	$35 < PM_{2.5} \leq 75$	$75 < PM_{2.5} \leq 115$	$PM_{2.5} > 115$
cold	38.1%	70.0%	91.7%
hot	61.9%	30.0%	8.3%

Table 2. The proportions of three O_3 levels ($\mu g \cdot m^{-3}$) in cold and hot seasons in the urban area of Nanjing over 2013–2015.

Seasons	$100 < O_3 \leq 160$	$160 < O_3 \leq 200$	$O_3 > 200$
cold	18.4%	0.0%	0.0%
hot	81.6%	100.0%	100.0%

It is shown in Tables 1 and 2 that haze pollution occurred mostly in cold winter with high proportions of 70.0% and 91.7% respectively in moderate and heavy $PM_{2.5}$ levels over 2013–2015 (Table 1). This was extreme in the case of O_3 pollution in hot summer, where the proportions of ambient O_3 levels reached up to 100% in moderate and heavy levels of photochemical air pollution (Table 2), determining the summertime air quality change in this urban region of East China, which is consistent with the seasonality of haze and photochemical air pollution in China [8,26].

Atmospheric environment change is generally controlled by air pollutant emissions and meteorological conditions [27–29]. To understand the meteorological drivers in the seasonal variations of ambient $PM_{2.5}$ and O_3, Figure 2 presented the diurnal changes of surface air temperature and total radiation in cold and hot seasons averaged over 2013–2015 with the seasonal averages of surface air temperature and total radiation (Table 3). Seasonally averaged over three years, the large difference in total radiation existed with the diurnal peaks of 1.07 $MJ \cdot m^{-2}$ and 2.00 $MJ \cdot m^{-2}$ as well as and the seasonal averages of 0.26 ± 0.53 $MJ \cdot m^{-2}$ and 0.66 ± 1.05 $MJ \cdot m^{-2}$ respectively in cold and hot seasons (Figure 2; Table 3). In cold season, surface air temperature was averaged with 5.2 °C, while 25.6 °C averaged in hot season. Strong (weak) atmospheric radiation and high (low) air temperature in hot (cold) season could be conducive (unconducive) to photochemical reactions for high O_3 production and atmospheric oxidation for secondary particle formation. Additionally, weak atmospheric radiation and low surface air temperature in cold season could potentially reduce the atmospheric boundary layer height and mixing, leading to $PM_{2.5}$ accumulations for increasing wintertime haze pollution in East China [26].

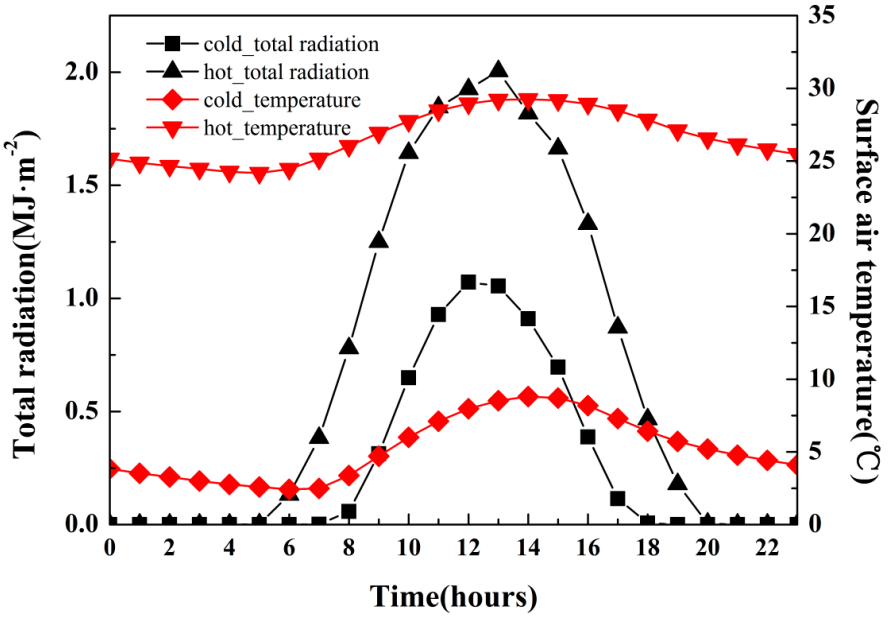

Figure 2. Diurnal changes of surface air temperature (°C) and total radiation (MJ·m^{-2}) in the local time in Nanjing averaged in cold and hot seasons over 2013–2015.

Table 3. Seasonal averages (±standard deviations) of air temperature (°C) and total radiation (MJ·m^{-2}) in Nanjing over 2013–2015.

Seasons	Surface Air Temperature (°C)	Total Radiation (MJ·m^{-2})
cold	5.2 ± 4.3	0.26 ± 0.53
hot	25.6 ± 4.2	0.66 ± 1.05

3.2. Strong Atmospheric Oxidation Promoting Secondary Particle Formation

In this study, we introduced OX (OX = O_3 + NO_2) to characterize the atmospheric oxidation ability [30–33]. The seasonally averaged OX concentrations in cold and hot seasons were 95.4 and 105.0 μg·m^{-3} respectively (Table 4), indicating high atmospheric oxidation in hot season with strong atmospheric radiation and high air temperature (Table 3). In cold season, the correlation coefficients of OX to NO_2 and O_3 were 0.68 and 0.14 respectively, and the ratio of O_3/OX was 0.36, manifesting a more important role of NO_2 in atmospheric oxidation. In hot season, the correlation coefficients of OX to O_3 and NO_2 were 0.95 and 0.49 with the ratio of O_3/OX of 0.61, which implied that O_3 could significantly promote the level of atmospheric oxidation in hot season.

Table 4. OX (OX = O_3 + NO_2) averages and ratios of O_3/OX as well as the correlations of OX to NO_2 and O_3 in cold and hot seasons over 2013–2015 in Nanjing.

Seasons	Average OX (μg·m^{-3})	O_3/OX Ratios	Correlation to NO_2	Correlation to O_3
cold	95.4	0.36	0.68 **	0.14 *
hot	105.0	0.61	0.49 **	0.95 **

* passing the significant levels $p < 0.05$; ** passing the significant levels $p < 0.01$.

The daily maximum concentration $O_{3\text{-max}}$ could usually be used to quantify the role of secondary particles in air quality change due to the close relation between secondary particle formation and photochemical activities through atmospheric oxidation [34–37]. CO could be regarded as a proxy of primary particles, and $O_{3\text{-max}}$ as photochemical activity index [38]. We adopted the method [38] to assess the contribution of secondary particle formation in different levels of atmospheric oxidation

based on daily $O_{3\text{-max}}$ concentrations from 2013 to 2015. In order to distinguish the effects of various degrees of photochemical activities, similarly to Table 2, the daily $O_{3\text{-max}}$ concentrations were categorized into three levels between 100 and 160 $\mu g \cdot m^{-3}$, between 160 and 200 $\mu g \cdot m^{-3}$, and greater than 200 $\mu g \cdot m^{-3}$. Under the low photochemical activities with daily $O_{3\text{-max}} < 100$ $\mu g \cdot m^{-3}$ for clean air, the observed hourly values of $PM_{2.5}/CO$ could be referred to a representative ratio of primary $PM_{2.5}$ particles for all scenarios with $(PM_{2.5}/CO)_{p,L,h}$, where p, L and h respectively denoted primary particles, low photochemical activities with daily $O_{3\text{-max}} < 100$ $\mu g \cdot m^{-3}$, and daytime in hours. Based on the ratio of $(PM_{2.5}/CO)_{p,L,h}$ and the hourly $PM_{2.5}$ and CO concentrations for light, moderate and heavy levels of photochemical activities, the mass concentrations of primary particles could be estimated with the following formulae:

$$(PM_{2.5})_{p,LH,h} = CO_{LH,h} \times (PM_{2.5}/CO)_{p,L,h} \quad (2)$$

$$(PM_{2.5})_{p,M,h} = CO_{M,h} \times (PM_{2.5}/CO)_{p,L,h} \quad (3)$$

$$(PM_{2.5})_{p,H,h} = CO_{H,h} \times (PM_{2.5}/CO)_{p,L,h} \quad (4)$$

where LH, M and H represented respectively the light, moderate and heavy levels of photochemical pollution ranked with 100 $\mu g \cdot m^{-3} < O_{3\text{-max}} \leq 160$ $\mu g \cdot m^{-3}$, 160 $\mu g \cdot m^{-3} < O_{3\text{-max}} \leq 200$ $\mu g \cdot m^{-3}$, and $O_{3\text{-max}} > 200$ $\mu g \cdot m^{-3}$ (Table 2).

The secondary particle concentrations in $PM_{2.5}$ could be estimated with the differences between the observed $PM_{2.5}$ concentrations and the primary $PM_{2.5}$ calculated with Equations (2)–(4) in each level of photochemical pollution as follows:

$$(PM_{2.5})_{sec,LH,h} = (PM_{2.5})_{obs,LH,h} - (PM_{2.5})_{p,LH,h} \quad (5)$$

$$(PM_{2.5})_{sec,M,h} = (PM_{2.5})_{obs,M,h} - (PM_{2.5})_{p,M,h} \quad (6)$$

$$(PM_{2.5})_{sec,H,h} = (PM_{2.5})_{obs,H,h} - (PM_{2.5})_{p,H,h} \quad (7)$$

where $(PM_{2.5})_{sec,LH,h}$, $(PM_{2.5})_{sec,M,h}$ and $(PM_{2.5})_{sec,H,h}$ were the estimated mass concentrations of secondary particles in light, moderate and heavy levels of photochemical pollution.

By employing the hourly observation data of $PM_{2.5}$, CO and O_3 in the urban area of Nanjing over 2013–2015, we estimated the mass concentrations of primary and secondary $PM_{2.5}$ particles with Equations (2)–(7) to assess the contributions of secondary $PM_{2.5}$ particles to ambient $PM_{2.5}$ in the light, moderate and heavy levels of photochemical pollution classified with 100 $\mu g \cdot m^{-3} < O_{3\text{-max}} \leq 160$ $\mu g \cdot m^{-3}$, 160 $\mu g \cdot m^{-3} < O_{3\text{-max}} \leq 200$ $\mu g \cdot m^{-3}$, and $O_{3\text{-max}} > 200$ $\mu g \cdot m^{-3}$, which was illustrated with the three-year averages over both cold and hot seasons in Figure 3. Under the light, moderate and heavy levels of photochemical air pollution, the secondary $PM_{2.5}$ particles could contribute 6.82%, 12.26% to 26.76% mass concentrations to ambient $PM_{2.5}$ particles. Considering the strong atmospheric radiation and high air temperature enhancing atmospheric oxidation in hot summer with high proportions of O_3 pollution reaching up to 100% in moderate and heavy levels (Figure 2; Tables 2–4), the augmentation of atmospheric oxidation could strengthen the production of secondary particles with the contribution up to 26.76% to ambient $PM_{2.5}$ levels. High O_3 concentrations in strong oxidative air condition during hot season promoted the formation of secondary particles, which could result in a positive correlation between $PM_{2.5}$ and O_3 in hot season.

It should be pointed out that the contributions of secondary $PM_{2.5}$ particles to air pollution were qualified by adopting the assessment approach of Chang et al. [38] to understand the positive correlation between $PM_{2.5}$ and O_3 during hot season in this study, which could reflect the role of atmospheric oxidation in secondary particle formation with the discrepancies from previous studies on other urban regions [19,39]. A complete understanding of the physical and chemical processes of secondary particle formation in the atmosphere, especially heterogeneous reactions on atmospheric

particles in changing meteorology, could improve the assessment on the contribution of secondary particles in air compound pollution.

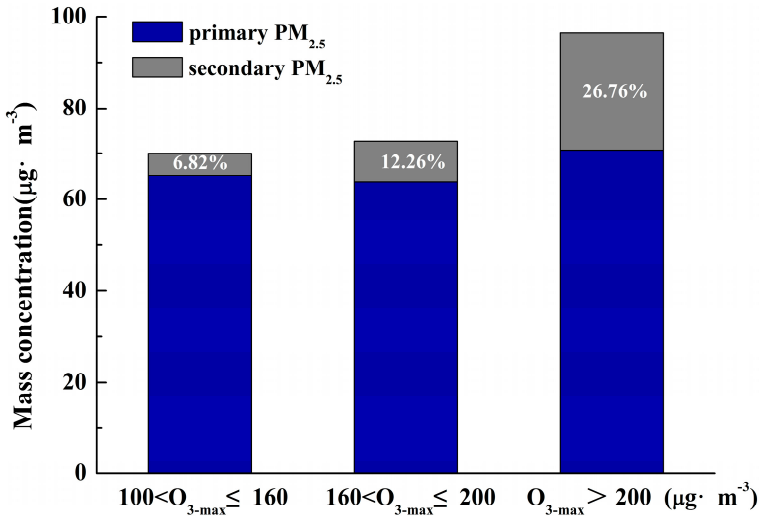

Figure 3. The contributions of secondary $PM_{2.5}$ particles to ambient $PM_{2.5}$ concentrations under photochemical activities ranged with 100 μg·m^{-3} < $O_{3\text{-max}}$ ≤ 160 μg·m^{-3}, 160 μg·m^{-3} < $O_{3\text{-max}}$ ≤ 200 μg·m^{-3}, and $O_{3\text{-max}}$ > 200 μg·m^{-3} estimated from the three-year environmental observation in the urban area of Nanjing.

3.3. High $PM_{2.5}$ Concentrations Suppressing Solar Radiation and O_3 Production

Major chemical components of $PM_{2.5}$ such as sulfate, nitrate, organic matter and elemental carbon all have strong ability of extinction [40,41]. Atmospheric particles can scatter and absorb ultraviolet radiation directly, altering the intensity of incident ultraviolet radiation to impact atmospheric oxidation and O_3 generation [42,43]. Atmospheric particulates could also affect atmospheric oxidation and O_3 formation by modifying cloud physical processes with the effective radius and concentrations of cloud droplets as well as the optical thickness of clouds [44–46].

In order to examine the effect of $PM_{2.5}$ on atmospheric radiation in the urban area of East China, the diurnal changes of total radiation were analyzed under light, moderate and heavy levels of $PM_{2.5}$ pollution ranged with daily $PM_{2.5}$ concentrations from 35 to 75 μg·m^{-3}, from 75 to 115 μg·m^{-3} and exceeding 115 μg·m^{-3} (Table 1), based on the meteorological and environmental observations over 2013–2015. Figure 4 presented the daily changes of the atmospheric total radiation averaged over the three years under the light, moderate and heavy levels of $PM_{2.5}$ mass concentrations. It is remarkable in Figure 4 that the magnitudes of total radiation were generally lower from light, moderate and heavy levels of $PM_{2.5}$ pollution; especially around noon, with the more significant decreases in total radiation, the total radiation peaks dropped from 1.823 MJ·m^{-2} in the light $PM_{2.5}$ pollution (35 μg·m^{-3} < $PM_{2.5}$ < 75 μg·m^{-3}), 1.303 MJ·m^{-2} in the moderate $PM_{2.5}$ pollution (35 μg·m^{-3} < $PM_{2.5}$ < 75 μg·m^{-3}) to 1.159 MJ·m^{-2} in the heavy $PM_{2.5}$ pollution ($PM_{2.5}$ > 115 μg·m^{-3}), which confirmed that the enhancing $PM_{2.5}$ levels could significantly reduce solar radiation in ambient atmosphere with strong radiative forcing.

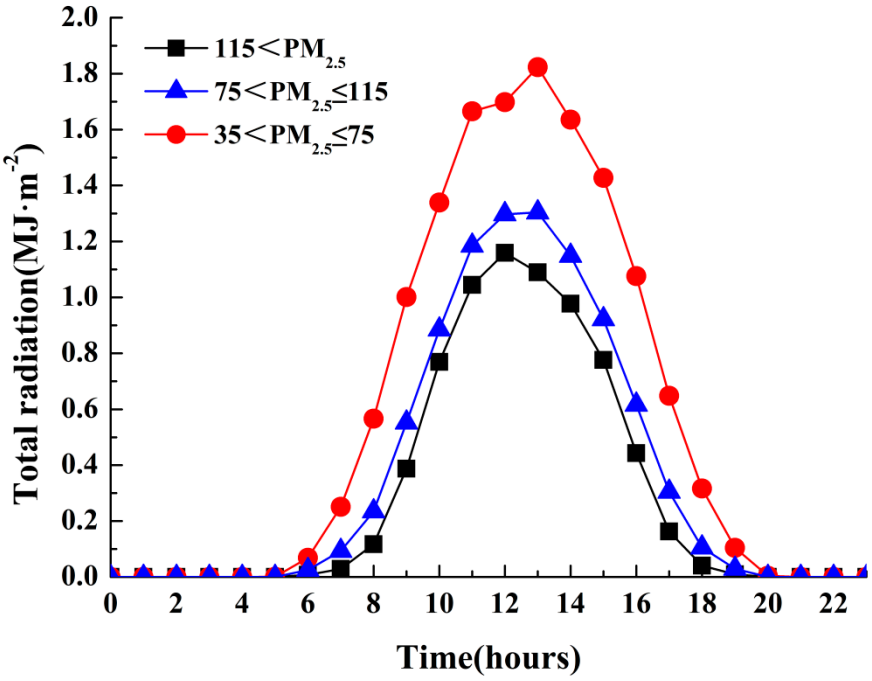

Figure 4. Diurnal changes of total radiation in local time under three $PM_{2.5}$ levels over 35–75 μg·m^{-3} and 75–115 μg·m^{-3} as well as exceeding 115 μg·m^{-3} during 2013–2015 in Nanjing.

The O_3 change rate could be estimated with the hourly difference of O_3 concentrations by using the hourly data of ambient O_3 measurements over the urban sites of Nanjing. To investigate the inhibitory effect of ambient $PM_{2.5}$ concentrations on O_3 generation by reducing solar total radiation in $PM_{2.5}$ polluted air (Figure 4), we averaged the O_3 change rates in the same levels to Figure 4 ranked with light $PM_{2.5}$ pollution (35 μg·m^{-3} < $PM_{2.5}$ ≤ 75 μg·m^{-3}), moderate $PM_{2.5}$ pollution (75 μg·m^{-3} < $PM_{2.5}$ ≤ 115 μg·m^{-3}) and heavy $PM_{2.5}$ pollution ($PM_{2.5}$ > 115 μg·m^{-3}) over 2013–2015. Figure 5 presented the diurnal distribution of O_3 change rates in light, moderate and heavy $PM_{2.5}$ pollution levels, where the positive and negative O_3 change rates respectively indicated O_3 generation and loss in ambient air. As shown in Figure 5, the daytime O_3 change rates decreased gradually, especially more significantly around noon with $PM_{2.5}$ pollution worsening from light, moderate and heavy levels. In accompany with light, moderate to heavy air pollution, daytime O_3 generation rates peaked respectively with 16.4 μg·m^{-3} h^{-1} at 11 a.m., 15.0 μg·m^{-3} h^{-1} at 12 a.m. to 12.7 μg·m^{-3} h^{-1} at 1 p.m. (Figure 5). The peaks of daytime O_3 change rates were lowered in the time delay of about one hour with enhancing $PM_{2.5}$ levels in the urban atmosphere. The increases of $PM_{2.5}$ concentrations could exert a significant inhibitory effect on ambient O_3 levels.

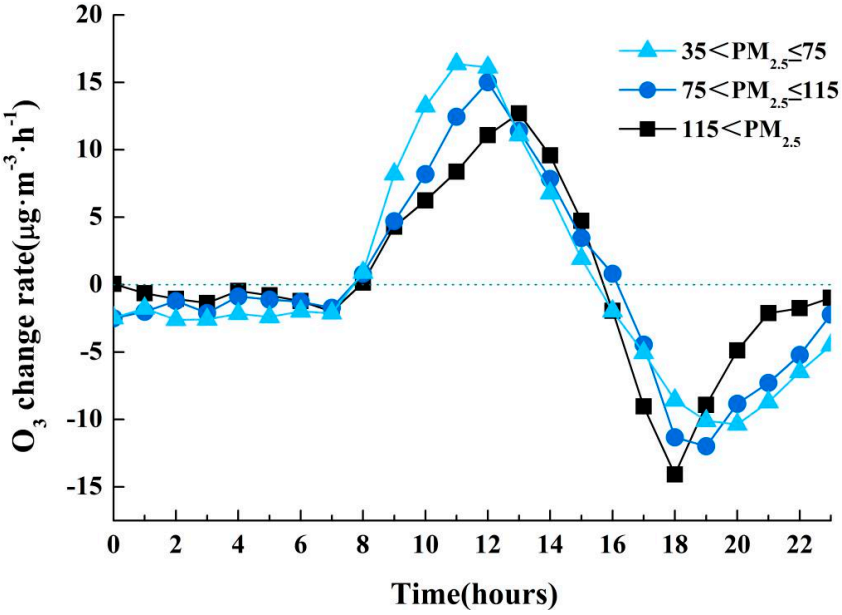

Figure 5. Diurnal distribution in local time of O_3 change rates under three $PM_{2.5}$ levels over 35−75 μg·m^{-3} and 75–115 μg·m^{-3} as well as exceeding 115 μg·m^{-3} during 2013–2015 in Nanjing.

High $PM_{2.5}$ pollution occurred mostly in cold season with the large proportions of 70.0% and 91.7% in the moderate (75 μg·m^{-3} < $PM_{2.5}$ ≤ 115 μg·m^{-3}) and heavy ($PM_{2.5}$ > 115 μg·m^{-3}) levels over 2013–2015 (Table 1), which could reduce solar total radiation and suppress O_3 production (Figures 4 and 5). Furthermore, the wintertime climate in Nanjing was featured with weak atmospheric radiation and low air temperature inhibiting photochemical reactions (Tables 3 and 4). The environmental and meteorological conditions could lead to a negative correlation between $PM_{2.5}$ and O_3 in seasonal air quality change. Wintertime $PM_{2.5}$ pollution could suppress ambient O_3 levels with reduction of atmospheric radiation, which dominated the interaction of $PM_{2.5}$ and O_3 in cold season.

4. Conclusions

Previous studies on interaction between $PM_{2.5}$ and O_3 were concentrated on individual seasons and air pollution events. This study analyzed the three-year (2013–2015) environmental and meteorological monitoring data in Nanjing, a major urban area in East China, and investigated the seasonal change in interaction of $PM_{2.5}$ and O_3 and the underlying mechanisms to comprehensively understand air compound pollution in China with the implications on atmospheric environment changes.

The inverse relations of ambient $PM_{2.5}$ and O_3 in atmospheric compound pollution between cold and hot seasons were evidenced in this study with three-year environmental observation in an urban area of East China. By analyzing the three-year observations of environment and meteorology, the underlying mechanisms on interaction of $PM_{2.5}$ and O_3 in atmospheric compound pollution were revealed with two processes (Figure 6): (1) high O_3 concentrations with strong atmospheric oxidation could promote the secondary particle formation enhancing ambient $PM_{2.5}$ levels; and (2) enhanced $PM_{2.5}$ concentrations could suppress ambient O_3 levels with reduction of atmospheric radiation. Processes 1 and 2 could build a cycle of interaction between air compound pollutants $PM_{2.5}$ and O_3. Under the different environmental and meteorological conditions in cold and hot seasons, processes 1 and 2 could respectively play a dominating role in interaction of $PM_{2.5}$ and O_3 during hot and cold seasons (Figure 6). Strong atmospheric oxidation promotes secondary particle formation in hot season, and high $PM_{2.5}$ concentrations suppresses solar radiation and O_3 production in cold season, which could lead to the negative and positive relations between ambient $PM_{2.5}$ and O_3 in

cold and hot seasons. The seasonal variation of air compound pollution could be determined by the seasonally changing interaction of $PM_{2.5}$ and O_3 in atmospheric environment.

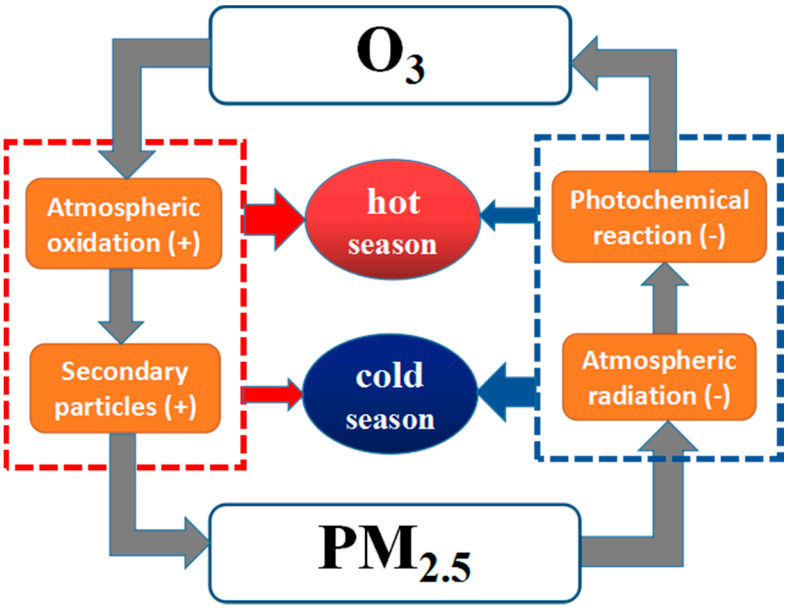

Figure 6. A diagram on the underlying mechanisms of inversion relations between ambient $PM_{2.5}$ and O_3 in the cold and hot seasons with (+) enhancing and (−) suppressing effects dominating (wide red and blue arrows) the interaction of $PM_{2.5}$ and O_3 in air compound pollution.

This study revealed the interaction of $PM_{2.5}$ and O_3 in air compound pollution, based on the three-year data from environmental and meteorological measurements over an urban area of East China. It should be emphasized that heterogeneous reactions occurring on particulate matters are an important means of interaction between O_3 and $PM_{2.5}$. The seasonal variations in meteorology (e.g., winds, atmospheric mixing conditions and precipitation) and air pollutant emissions, especially biogenic VOC emissions, could also influence the interaction of O_3 and $PM_{2.5}$, which could be important issues in further study on atmospheric environment change.

Acknowledgments: This work was jointly funded by National Key R & D Program Pilot Projects of China (2016YFC0203304), Chinese National Science-Technology Support Plan (2014BAC22B04), National Natural Science Foundation of China (41375140) and Jiangsu province Environmental science research project (2015017), as well as the Special Fund for Environment Scientific Research in the Public Interest (201509001) and the Fundamental Research Funds from Chinese Academy of Meteorological Sciences (2016Y005). The ESMC publication number is 155. We thank Integrated Observatory Training Base of China Meteorological Administration (Nanjing) for providing total radiation data.

Author Contributions: Mengwei Jia and Tianliang Zhao conceived and designed the experiments as well as writing the article; Xinghong Cheng and Sunling Gong conceived and designed the experiments; Xiangzhi Zhang, Lili Tang and Duanyang Liu analyzed the data; Mengwei Jia and Xianghua Wu performed the experiments; Liming Wang and Yusheng Chen helped perform the statistical analysis.

Conflicts of Interest: The authors declare no conflict of interest.

References

1. Chen, X.; Zhang, L.W.; Huang, J.J.; Song, F.J.; Zhang, L.P.; Qian, Z.M.; Trevathan, E.; Mao, H.J.; Han, B.; Vaughn, M.; et al. Long-term exposure to urban air pollution and lung cancer mortality: A 12-year cohort study in Northern China. *Sci. Total Environ.* **2016**, *571*, 855–861. [CrossRef] [PubMed]
2. Fang, D.; Wang, Q.; Li, H.; Yu, Y.; Yan, L.; Xin, Q. Mortality effects assessment of ambient $PM_{2.5}$ pollution in the 74 leading cities of China. *Sci. Total Environ.* **2016**, *s569–s570*, 1545–1552. [CrossRef] [PubMed]
3. Parrish, D.D.; Zhu, T. Clean air for megacities. *Science* **2009**, *326*, 674–675. [CrossRef] [PubMed]

4. Tie, X.; Cao, J. Aerosol Pollution in China: Present and Future Impact on Environment. *Particuology* **2009**, *7*, 426–431. [CrossRef]
5. Zhang, Y.H.; Hu, M.; Zhong, L.J.; Wiedensohler, A.; Liu, S.C.; Andreae, M.O.; Wang, W.; Fan, S.J. Regional Integrated Experiments on Air Quality over Pearl River Delta 2004 (PRIDE-PRD2004): Overview. *Atmos. Environ.* **2008**, *42*, 6157–6173. [CrossRef]
6. Tie, X.; Wu, D.; Brasseur, G. Lung cancer mortality and exposure to atmospheric aerosol particles in Guangzhou, China. *Atmos. Environ.* **2009**, *43*, 2375–2377. [CrossRef]
7. Wang, Y.Q.; Zhang, X.Y.; Sun, J.Y.; Zhang, X.C.; Che, H.Z.; Li, Y. Spatial and temporal variations of the concentrations of PM_{10}, $PM_{2.5}$ and PM_1 in China. *Atmos. Chem. Phys.* **2015**, *15*, 15319–15354. [CrossRef]
8. Xiao, Z.M.; Zhang, Y.F.; Hong, S.M.; Bi, X.H.; Jiao, L.; Feng, Y.C.; Wang, Y.Q. Estimation of the Main Factors Influencing Haze, Based on a Long-term Monitoring Campaign in Hangzhou, China. *Aerosol Air Qual. Res.* **2011**, *11*, 873–882. [CrossRef]
9. Leng, C.P.; Duan, J.Y.; Xu, C.; Zhang, H.F.; Wang, Y.F.; Wang, Y.Y.; Li, X.; Kong, L.D.; Tao, J.; Zhang, R.J.; et al. Insights into a historic severe haze weather in Shanghai: Synoptic situation, boundary layer and pollutants. *Atmos. Chem. Phys.* **2015**, *15*, 32561–32605. [CrossRef]
10. Ma, Z.Q.; Xu, J.; Quan, W.J.; Zhang, Z.Y.; Lin, W.L. Significant increase of surface ozone at a regional background station in the eastern China. *Atmos. Chem. Phys. Discuss.* **2015**, *15*, 31951–31972. [CrossRef]
11. Ma, J.Z.; Xu, X.B.; Zhao, C.; Yan, P. A Review of Atmospheric Chemistry Research in China: Photochemical Smog, Haze Pollution, and Gas-Aerosol Interactions. *Adv. Atmos. Sci.* **2012**, *29*, 1006–1026. [CrossRef]
12. Meng, Z.; Dabdub, D.; Seinfeld, J.H. Chemical coupling between atmospheric ozone and particulate matter. *Science* **1997**, *277*, 116–119. [CrossRef]
13. Ravishankara, A.R. Heterogeneous and Multiphase Chemistry in the Troposphere. *Science* **1997**, *276*, 1058–1065. [CrossRef]
14. Jacob, D.J. Heterogeneous chemistry and tropospheric ozone. *Atmos. Environ.* **2000**, *34*, 2131–2159. [CrossRef]
15. Li, G.; Zhang, R.; Fan, J.; Tie, X. Impacts of black carbon aerosol on photolysis and ozone. *J. Geophys. Res. Atmos.* **2005**, *110*, 3233–3250. [CrossRef]
16. Li, J.; Wang, Z.; Wang, X.; Yamaji, K.; Takigawa, M.; Kanaya, Y.; Pochanart, P.; Liu, Y.; Irie, H.; Hu, B.; et al. Impacts of aerosols on summertime tropospheric photolysis frequencies and photochemistry over Central Eastern China. *Atmos. Environ.* **2011**, *45*, 1817–1829. [CrossRef]
17. Li, L.; Chen, Z.M.; Zhang, Y.H.; Zhu, T.; Li, J.L.; Ding, J. Kinetics and mechanism of heterogeneous oxidation of sulfur dioxide by ozone on surface of calcium carbonate. *Atmos. Chem. Phys.* **2006**, *6*, 125–139. [CrossRef]
18. Ge, B.; Sun, Y.; Liu, Y.; Dong, H.; Ji, D.; Jiang, Q.; Li, J.; Wang, Z. Nitrogen Dioxide Measurement by Cavity Attenuated Phase Shift Spectroscopy (CAPS) and Implications in Ozone Production Efficiency and Nitrate Formation in Beijing, China. *J. Geophys. Res.* **2013**, *118*, 9499–9509. [CrossRef]
19. Huang, R.J.; Zhang, Y.; Bozzetti, C.; Ho, K.F.; Cao, J.J.; Han, Y.; Daellenbach, K.R.; Slowik, J.G.; Platt, S.M.; Canonaco, F. High secondary aerosol contribution to particulate pollution during haze events in China. *Nature* **2014**, *514*, 218–222. [CrossRef] [PubMed]
20. Haywood, J.; Boucher, O. Estimates of the direct and indirect radiative forcing due to tropospheric aerosols: A review. *Rev. Geophys.* **2000**, *38*, 513–543. [CrossRef]
21. Zhu, S.; Butler, T.; Sander, R.; Ma, J.; Lawrence, M.G. Impact of dust on tropospheric chemistry overpolluted regions: A case study of the Beijing megacity. *Atmos. Chem. Phys.* **2010**, *10*, 3855–3873. [CrossRef]
22. Xu, J.; Zhang, Y.H.; Wang, W. Numerical study on the impacts of heterogeneous reactions on ozone formation in the Beijing urban area. *Adv. Atmos. Sci.* **2006**, *23*, 605–614. [CrossRef]
23. Feng, T.; Bei, N.; Huang, R.J.; Cao, J.; Zhang, Q.; Zhou, W.; Tie, X.; Liu, S.; Zhang, T.; Su, X.; et al. Summertime ozone formation in Xi'an and surrounding areas, China. *Atmos. Chem. Phys. Discuss.* **2015**, *15*, 30563–30608. [CrossRef]
24. Ding, Y. Monsoons over China. *Adv. Atmos. Sci.* **1994**, *11*, 252.
25. Shao, M.; Wang, S.; Russell, A.G. Air pollution complex: Understanding the sources, formation processes and health effects. *Front. Environ. Sci. Eng.* **2016**, *10*, 20. [CrossRef]
26. Xu, X.; Zhao, T.; Liu, F.; Gong, S.L.; Kristovich, D.; Lu, C.; Guo, Y.; Cheng, X.; Wang, Y.; Ding, G. Climate modulation of the Tibetan Plateau on haze in China. *Atmos. Chem. Phys.* **2015**, *15*, 28915–28937. [CrossRef]
27. Jacob, D.J.; Winner, D.A. Effect of Climate Change on Air Quality. *Atmos. Environ.* **2009**, *43*, 51–63. [CrossRef]

28. Ebi, K.; Mcgregor, G. Climate change, tropospheric ozone and particulate matter, and health impacts. *Ciênc. Saúde Coletiva* **2008**, *116*, 1449–1455. [CrossRef] [PubMed]
29. Wang, H.J.; Chen, H.P. Understanding the recent trend of haze pollution in eastern China: Roles of climate change. *Atmos. Chem. Phys.* **2016**, *16*, 1–18. [CrossRef]
30. Clapp, L.J.; Jenkin, M.E. Analysis of the relationship between ambient levels of O_3, NO_2, and NO as a function of NOx, in the UK. *Atmos. Environ.* **2001**, *35*, 6391–6405. [CrossRef]
31. Stephens, S.; Madronich, S.; Wu, F.; Olson, J.B. Weekly patterns of México City's surface concentrations of CO, NOx, PM_{10} and O_3 during 1986–2007. *Atmos. Chem. Phys.* **2008**, *8*, 5313–5325. [CrossRef]
32. Cheung, V.T.; Wang, T. Observational study of ozone pollution at a rural site in the Yangtze Delta of China. *Atmos. Environ.* **2001**, *35*, 4947–4958. [CrossRef]
33. Zhang, W.; Capps, S.L.; Hu, Y.; Nenes, A. Development of the high-order decoupled direct method in three dimensions for cparticulate matter: Enabling advanced sensitivity analysis in air quality models. *Geosci. Model Dev. Discuss.* **2011**, *5*, 355–368. [CrossRef]
34. Na, K.; Sawant, A.; Song, C.; Cocker, D. Primary and secondary carbonaceous species in the atmosphere of Western Riverside County, California. *Atmos. Environ.* **2004**, *38*, 1345–1355. [CrossRef]
35. Grosjean, D. Organic acids in Southern California air: Ambient concentrations, mobile source emissions, in situ formation and removal processes. *Environ. Sci. Technol.* **1989**, *23*, 1506–1514. [CrossRef]
36. Rodriguez, S.; Querol, X.; Alastuey, A.; Mantilla, E. Origin of high summer PM_{10} and TSP concentrations at rural sites in Eastern Spain. *Atmos. Environ.* **2002**, *36*, 3101–3112. [CrossRef]
37. Turpin, B.J.; Huntzicker, J.J. Identification of secondary organic aerosol episodes and quantitation of primary and secondary organic aerosol concentrations during SCAQS. *Atmos. Environ.* **1995**, *29*, 3527–3544. [CrossRef]
38. Chang, S.C.; Lee, C.T. Secondary aerosol formation through photochemical reactions estimated by using air quality monitoring data in Taipei City from 1994 to 2003. *Atmos. Environ.* **2007**, *41*, 4002–4017. [CrossRef]
39. Dawson, J.P.; Bloomer, B.J.; Winner, D.A.; Weaver, C.P. Understanding the Meteorological Drivers of U.S. Particulate Matter Concentrations in a Changing Climate. *Bull. Am. Meteorol. Soc.* **2014**, *95*, 521–532. [CrossRef]
40. John, G.W. Visibility: Science and regulation. *J. Air Waste Manag. Assoc.* **2002**, *52*, 628–713.
41. Tao, J.; Zhang, L.; Ho, K.; Zhang, R.; Lin, Z.; Zhang, Z.; Lin, M.; Cao, J.; Liu, S.; Wang, G. Impact of $PM_{2.5}$, chemical compositions on aerosol light scattering in Guangzhou—The largest megacity in South China. *Atmos. Res.* **2014**, *135–136*, 48–58. [CrossRef]
42. Dickerson, R.R.; Kondragunta, S.; Stenchikov, G.; Civerolo, K.L.; Doddridge, B.G.; Holben, B.N. The impact of aerosols on solar ultraviolet radiation and photochemical smog. *Science* **1997**, *278*, 827. [CrossRef] [PubMed]
43. Li, G.; Bei, N.; Tie, X.; Molina, L.T. Aerosol effects on the photochemistry in Mexico City during MCMA-2006/MILAGRO campaign. *Atmos. Chem. Phys.* **2011**, *11*, 5169–5182. [CrossRef]
44. Twomey, S. Pollution and the planetary albedo. *Atmos. Environ.* **2007**, *8*, 1251–1256. [CrossRef]
45. Menon, S.; Unger, N.; Koch, D.; Francis, J.; Garrett, T.; Sednev, I.; Shindell, D.; Streets, D. Aerosol climate effects and air quality impacts from 1980 to 2030. *Environ. Res. Lett.* **2008**, *3*, 024004. [CrossRef]
46. Unger, N.; Menon, S.; Shindell, D.T.; Koch, D.M. Impacts of aerosol indirect effect on past and future changes in tropospheric composition. *Atmos. Chem. Phys. Discuss.* **2009**, *9*, 4115–4129. [CrossRef]